NATIONAL ADVISORY COMMITTEE FOR AERONAUTICS

TECHNICAL NOTE 1906

AN ANALYTICAL STUDY OF THE STEADY VERTICAL DESCENT IN AUTOROTATION OF SINGLE-ROTOR HELICOPTERS

By A. A. Nikolsky and Edward Seckel

Princeton University

Washington

June 1949

NATIONAL ADVISORY COMMITTEE FOR AERONAUTICS

TECHNICAL NOTE 1906

AN ANALYTICAL STUDY OF THE STEADY VERTICAL DESCENT IN AUTOROTATION OF SINGLE-ROTOR HELICOPTERS

By A. A. Nikolsky and Edward Seckel

SUMMARY

A detailed analysis of steady autorotative vertical descent of a helicopter is made, in which the effect of considering induced velocity constant over the disk is examined. The induced velocity is first considered constant, then variable over the disk; and the results are compared for a typical helicopter. Although considering the induced velocity constant over the disk causes considerable error in the load distribution along a blade, the revolutions per minute of the rotor and rate of descent are found to be negligibly affected for small angles of blade pitch. For high pitch angles, where blade stalling becomes important, the theoretical difference between blade load distributions obtained by considering induced velocity constant and variable may be expected to be enough to cause quantitative disagreement between the constant induced-velocity theory and experiment.

A brief study is made of the stability of autorotation, considering the effect of blade stalling. At small values of blade incidence, stability of the autorotation will be adequate, and blade stalling can be neglected. As the blade incidence increases, the risk of an upgust causing the blades to stall and the rotor to stop becomes acute.

INTRODUCTION

This report is the result of the first part of a broad program to analyze the transient motions of a helicopter, which occur in the various phases of flight following power failure. As such, it is proper that it be concerned with steady-state vertical flight without power, or steady autorotative descent.

The basis for the analysis is contained in a paper by Glauert (reference 1), although a somewhat similar approach was made by Bennett in reference 2. There is no theory adequate to analyze the states of a rotor in autorotative vertical descent, and recourse must be made to an empirical relationship between the velocity of descent and total flow through the rotor disk. As more experimental evidence becomes available,

it will be possible to modify the necessary empiricisms to improve the agreement between analysis and fact.

This work was conducted at Princeton University under the sponsorship and with the financial assistance of the National Advisory Committee for Aeronautics.

SYMBOLS

Physical Quantities

W	gross weight, pounds
b	number of blades per rotor
R	blade radius, feet
r	radial distance to blade element, feet
$x = r/R$	
c	blade-section chord, feet
c_e	equivalent blade chord, feet $\left(c_e = \frac{\int_0^R cr^2 dr}{\int_0^R r^2 dr}\right)$
σ_x	blade-section solidity ratio $\left(\frac{bc}{\pi R}\right)$
σ	rotor solidity ratio $\left(\frac{bc_e}{\pi R}\right)$
θ	blade-section pitch angle from zero lift, radians unless otherwise stated
θ_0	blade pitch angle at hub
θ_1	linear twist of blade $\left(\theta = \theta_0 + \theta_1 x\right)$
S	disk area, square feet $\left(\pi R^2\right)$
ρ	mass density of air, slugs per cubic foot

Air-Flow Parameters

V	true airspeed of helicopter along flight path, feet per second
V_v	vertical component of V (positive down)
Ω	rotor angular velocity, radians per second
v	induced inflow velocity at rotor (always positive), feet per second
λ_x	inflow ratio at a blade element $\left(\frac{V_v - v}{\Omega R} = \frac{U_P}{\Omega R}\right)$
U	resultant velocity of the air relative to a blade element, perpendicular to blade-span axis, feet per second
U_P	component of U perpendicular to axis of no feathering (positive up toward rotor)
α_r	blade-section angle of attack from zero lift, radians unless otherwise stated
λ	inflow ratio with induced velocity assumed constant over the disk $\left(\frac{u}{\Omega R}\right)$
u	average value of U_P over disk (when induced velocity is assumed constant over the disk), feet per second (positive up)

Blade-Element Aerodynamic Characteristics

c_l	section lift coefficient
c_{d_o}	section profile-drag coefficient
$\delta_0,\delta_1,\delta_2,\delta_3$	coefficients in power series for c_{d_o} as a function of α_r $(c_{d_o} = \delta_0 + \delta_1\alpha_r + \delta_2\alpha_r^2 + \delta_3\alpha_r^3 + \cdots)$
c_{d_o}'	c_{d_o} corrected to account for friction torque
δ_0'	δ_0 corrected to account for friction torque

$\Delta\delta_0$ increment in δ_0 to account for friction torque

$(\delta_0' = \delta_0 + \Delta\delta_0)$

where

$$Q_f = -\frac{\rho}{2} b\Omega^2 R^4 (\Delta\delta_0) \int_0^1 cx^3 dx$$

$$c_{d_o}' = \delta_0' + \delta_1\alpha_r + \delta_2\alpha_r^2 + \delta_3\alpha_r^3 + \cdots$$

a slope of lift curve for blade, per radian $\left(\frac{dc_l}{d\alpha_r}\right)$

$c_{l_{max}}$ maximum section lift coefficient

x_s blade station inboard of which blade is stalled

c_{l_s} lift coefficient of stalled blade section

δ_s profile-drag coefficient of stalled blade section

F section thrust coefficient based on resultant velocity $\left(F = \frac{1}{4\pi r\rho U_p^2}\left(\frac{dT}{dr}\right)\right)$

f section thrust coefficient based on descending velocity $\left(f = \frac{1}{4\pi r\rho V_v^2}\left(\frac{dT}{dr}\right)\right)$

Rotor Aerodynamic Characteristics

T rotor thrust, pounds

Q rotor aerodynamic torque, pound-feet

Q_f rotor friction torque, pound-feet (may include torque to drive auxiliary mechanisms)

C_T rotor thrust coefficient $\left(C_T = \frac{T}{\pi\rho R^2(\Omega R)^2}\right)$

C_Q rotor torque coefficient $\left(C_Q = \frac{Q}{\pi\rho R^3(\Omega R)^2}\right)$

$\overline{F}$ rotor thrust coefficient based on resultant velocity $\left(\overline{F} = \frac{T}{2\pi\rho R^2 u^2}\right)$

$\overline{f}$ rotor thrust coefficient based on descending velocity $\left(\overline{f} = \frac{T}{2\pi\rho R^2 V_v^2}\right)$

Miscellaneous

K constant in empirical relation between f and F $\left(\frac{1}{f} = 2 \pm K\frac{1}{F}\right)$

$$p_1 = \left(\frac{V}{\Omega R}\right)^2 \frac{4}{a\sigma_x\theta}$$

$$p_2 = \frac{a\sigma_x}{8K}$$

$$p_3 = \frac{16K\theta}{a\sigma_x}$$

$$c_1 = \frac{2C_T}{a\sigma}\Omega^2 = \frac{2}{a\sigma\rho R^2}\left(\frac{T}{S}\right)$$

$$c_2 = \frac{1}{c_e}\int_0^1 c\theta x^2 dx$$

$$c_3 = \frac{1}{c_e}\int_0^1 cx\, dx$$

$$c_4 = \frac{2C_Q}{\sigma}\Omega^2$$

$$c_5 = -\frac{1}{c_e}\int_0^1 cx^3(\delta_0' + \delta_1\theta + \delta_2\theta^2)dx$$

$$c_6 = ac_2 - \frac{1}{c_e}\int_0^1 cx^2(\delta_1 + 2\delta_2\theta)dx$$

$$c_7 = c_3(a - \delta_2)$$

C_4, C_3, C_2, C_1, C_0 coefficients in power series for $\frac{2C_Q}{\sigma}$ as a function of λ $\left(\frac{2C_Q}{\sigma} = C_0 + C_1\lambda + C_2\lambda^2 + C_3\lambda^3 + C_4\lambda^4\right)$

METHOD OF ANALYSIS

The Relation between $\frac{1}{\bar{f}}$ and $\frac{1}{\bar{F}}$

It was shown by Lock in reference 3 that, for small values of resultant axial air velocity u through a rotor disk, the vortex and momentum theories are inapplicable. A relationship between u and the vertical component of descending velocity V_V was found experimentally and presented in terms of nondimensional coefficients $\bar{F}$ and $\bar{f}$ by Glauert in reference 1. The relation between $\bar{F}$ and $\bar{f}$ given by Glauert is given in figure 1 of this report (the solid line). The upper branch of the curve is for the windmill brake state, $u > 0$ (in which the rotor operates as a windmill, the average flow through the rotor being in the direction of the free stream); the lower branch is for the vortex ring state, $u < 0$ (in which the actual flow through the rotor is turbulent, at some places being in the direction of the free stream, and at some against. On the average, however, the flow through the rotor is against the free stream).

In order to simplify the analytical treatment, and because there is some doubt as to the exact relationship between $\bar{f}$ and $\bar{F}$, it is assumed in this report that the relationship is of the form

$$\frac{1}{\bar{f}} = 2 \pm K\frac{1}{\bar{F}} \qquad (1)$$

which is illustrated in figure 1 for $K = 1$ and 2. The upper branches (corresponding to the plus sign) are again for the windmill brake state, $u > 0$; the lower (for the minus sign) are for the vortex ring state, $u < 0$.

In this report, K will usually be taken as 2, so that, in hovering $\left(\frac{1}{\bar{f}} = 0\right)$, $\frac{1}{\bar{F}} = 1$, to agree with the vortex theory which is known to be reasonably accurate in its application to hovering. The effect of the different assumptions for $\frac{1}{\bar{f}}$ against $\frac{1}{\bar{F}}$ on descending velocity in steady autorotation is presented in figure 2, for a sample helicopter (see SAMPLE CALCULATIONS) with various blade incidences. It is seen that the differences are not large.

Derivation of the Equations

It is now assumed that the same relationship that exists between $\bar{f}$ and $\bar{F}$, for the rotor, exists as well between the corresponding coefficients f and F for any blade section, where, however, f and F are variable over the disk.

Considering now any blade section, from the definitions of f and F, there can be written

$$\frac{f}{F} = \left(\frac{U_P}{V_V}\right)^2 \tag{2}$$

and combining equations (1) and (2),

$$2f = 1 \mp K\left(\frac{U_P}{V_V}\right)^2 \tag{3}$$

where, in equation (3) and hereafter, the upper sign corresponds to the upper branch of $\frac{1}{f}$ against $\frac{1}{F}$ (the windmill brake state) and the lower sign to the lower branch of $\frac{1}{f}$ against $\frac{1}{F}$ (the vortex ring state).

Substituting in equation (3) the definition of f, and, since only vertical flight is concerned, dropping the subscript v on V_V,

$$\frac{dT}{dx} = 2\pi\rho x R^2\left(V^2 \mp KU_P{}^2\right) \tag{4}$$

From blade-element considerations,

$$\frac{dT}{dx} = \frac{\rho}{2} abcx^2\Omega^2R^3\left(\theta + \frac{U_P}{x\Omega R}\right) \tag{5}$$

Combining with equation (4) and letting

$$\left.\begin{aligned} p_1 &= \left(\frac{V}{\Omega R}\right)^2 \frac{4}{a\sigma_x\theta} \\ p_2 &= \frac{a\sigma_x}{8K} \\ p_3 &= \frac{16K\theta}{a\sigma_x} \\ \lambda_x &= \frac{U_P}{\Omega R} \end{aligned}\right\} \tag{6}$$

there results, for the two states

$$\lambda_x^2 \pm 2p_2\lambda_x \mp p_2^2 p_3(p_1 - x) = 0 \tag{7}$$

For the windmill brake state, $U_P > 0$, $\lambda_x > 0$, and the solution must be

$$\lambda_x = -p_2\left[1 - \sqrt{1 + p_3(p_1 - x)}\right] \tag{8}$$

and it must be that $x < p_1$.

For the vortex ring state, $U_P < 0$, $\lambda_x < 0$, and the solution must be

$$\lambda_x = p_2\left[1 - \sqrt{1 - p_3(p_1 - x)}\right] \tag{8a}$$

and it must be that $x > p_1$.

It is apparent then, that blade elements inboard of station $x = p_1$ are in the windmill brake state where the upper branch of $\frac{1}{f}$ against $\frac{1}{F}$ applies, and that blade elements outboard of station $x = p_1$ are in the vortex ring state, where the lower branch of $\frac{1}{f}$ against $\frac{1}{F}$ applies. At station $x = p_1$, $\lambda_x = U_P = 0$.

For steady autorotation, the thrust and torque equations are well known:

$$W = T = \frac{\rho}{2} ba\Omega^2 R^3 \int_0^1 c\left(\theta + \frac{\lambda_x}{x}\right)x^2 dx \tag{9}$$

and

$$Q = 0 = \frac{\rho}{2} b\Omega^2 R^4 \left[\int_0^1 ac\left(\theta + \frac{\lambda_x}{x}\right)\lambda_x x^2 dx - \int_0^1 cx^3\left(\delta_0' + \delta_1\theta + \delta_2\theta^2\right)dx - \int_0^1 cx^2\lambda_x\left(\delta_1 + 2\theta\delta_2\right)dx - \int_0^1 c\delta_2 x\lambda_x^2 dx\right] \tag{10}$$

in which the drag coefficient is represented by the series

$$c_{d_o}' = \delta_0' + \delta_1\alpha_r + \delta_2\alpha_r^2$$

The solution of these equations involves the determination, by trial and error, of the ratio $\frac{V}{\Omega R}$ such that the computed distribution of λ_x (equations (8) and (8a)) satisfies the torque equation.

Solution with Variable Induced Velocity

Steps in the solution of equations (8), (9), and (10) are outlined below:

(1) Assume a value for $\frac{V}{\Omega R}$, or compute an approximate value by assuming induced velocity constant over the disk by the method given in the following section.

(2) Choose a number of stations, such as $x = 0.2$, 0.4, 0.6, 0.8, and 1.0, and calculate at each station the values of p_1, p_2, and p_3 from equations (6).

(3) Calculate λ_x at each station, from equation (8) where $x < p_1$, or from equation (8a) where $x > p_1$.

(4) Substitute the values of λ_x into equation (10) and evaluate the integrals graphically or by Simpson's rule. Equation (10) must be satisfied. If it is not, a different value of $\frac{V}{\Omega R}$ should be assumed, and steps (1) through (4) repeated until the torque is substantially zero. Starting with the value of $\frac{V}{\Omega R}$ from constant induced-velocity considerations will lead usually to an accurate determination of $\frac{V}{\Omega R}$ for zero torque in three trials. The final value of $\frac{V}{\Omega R}$ will usually be between 0 and 10 percent larger than that for constant induced velocity.

(5) Having found the value of $\frac{V}{\Omega R}$ for zero torque, by trial and error in step (4), substitute the appropriate values of λ_x into equation (9), and evaluate the integral graphically or by Simpson's rule. Solve equation (9) for Ω.

(6) From the value of $\frac{V}{\Omega R}$ from step (4), and Ω from step (5), solve for the descending velocity V.

Solution with Induced Velocity Assumed Constant over the Disk

If it is assumed that the induced velocity is constant over the disk, then an approximate solution of the above equations can readily be obtained analytically. In this case λ_x is a constant λ; and the thrust and torque equations can be written

$$c_1 = \Omega^2\left(c_2 + c_3\lambda\right) \tag{11}$$

and

$$c_4 = \Omega^2\left(c_5 + c_6\lambda + c_7\lambda^2\right) \tag{12}$$

where

$$c_1 = \frac{2c_T}{a\sigma}\Omega^2 = \frac{2}{a\rho R^2\sigma}\left(\frac{T}{S}\right) \tag{13}$$

$$c_2 = \frac{1}{c_e}\int_0^1 c\theta x^2 dx \tag{13a}$$

$$c_3 = \frac{1}{c_e}\int_0^1 cx\,dx \tag{13b}$$

$$c_4 = \frac{2c_Q}{\sigma}\Omega^2 \tag{13c}$$

$$c_5 = -\frac{1}{c_e}\int_0^1 cx^3\left(\delta_0' + \delta_1\theta + \delta_2\theta^2\right)dx \tag{13d}$$

$$c_6 = ac_2 - \frac{1}{c_e}\int_0^1 cx^2\left(\delta_1 + 2\delta_2\theta\right)dx \tag{13e}$$

$$c_7 = c_3\left(a - \delta_2\right) \tag{13f}$$

In steady autorotation, the torque equals zero $\left(c_4 = 0\right)$, so that equation (12) reduces to

$$c_7\lambda^2 + c_6\lambda + c_5 = 0 \tag{14}$$

Since, with induced velocity constant, it must be assumed that the rotor is in the windmill brake state $(\lambda > 0)$, the solution must be

$$\lambda = \frac{-c_6 + \sqrt{c_6^2 - 4c_5c_7}}{2c_7} \tag{14a}$$

The following sequence may then be set down for solving the problem under the assumption of constant induced velocity:

(1) Calculate the coefficients c_1, c_2, c_3, c_4, c_5, c_6, and c_7 from equations (13) through (13f)

(2) Calculate λ from equation (14a)

(3) Calculate Ω from equation (11)

(4) Calculate u from the definition of λ $(u = \lambda\Omega R)$

(5) Calculate $\overline{F}$ from its definition $\left(\overline{F} = \frac{T}{2\pi\rho R^2 u^2}\right)$

(6) Calculate $\overline{f}$ from equation (1), using the plus sign (for the windmill brake state)

(7) From the definition of $\overline{f}$, calculate V $\left(V = \sqrt{\frac{T}{2\pi\rho R^2 \overline{f}}}\right)$

Stability of Autorotation

Blade element.— Considering, for the moment, the stability of a solitary blade element in autorotative vertical descent, the autorotation will be said to be stable, if, following a disturbance from the equilibrium condition of torque equal to zero, the blade element tends to return to the same equilibrium state. If the disturbance made the torque decelerating, say, then

(1) Ω would decrease

(2) dT and v would decrease

(3) V would increase

(4) Hence λ_x would increase

If the slope of dQ against λ_x, $\frac{\partial(dQ)}{\partial\lambda_x}$, were positive (torque becoming more autorotative for an increase in λ_x), then the equilibrium $(dQ = 0)$ would tend to be restored, and the autorotation would be stable. Conversely, if $\frac{\partial(dQ)}{\partial\lambda_x} < 0$, the autorotation would be unstable.

Rotor.— The criterion for the stability of the rotor as a whole, by extension of that for the blade element, is

$$\int_0^1 \frac{\partial\left(\frac{dQ}{dx}\right)}{\partial\lambda_x} dx > 0$$

Although the evaluation of the above integral is prohibitively difficult considering variable induced velocity, under the assumption of constant induced velocity over the disk, it reduces to

$$\frac{\partial Q}{\partial\lambda} > 0$$

It may be noted that for $\lambda = 0$, the torque would be negative (decelerating) for any pitch θ, so that, at the first trim point $(Q = 0)$ on a curve of Q against λ, $\frac{\partial Q}{\partial \lambda}$ must be positive. Therefore, for infinitesimal disturbances from this trim condition, the autorotation would be stable. As λ increases, however, beyond the first trim point, the angle of attack of the blades increases, until the blades stall, and the curve of Q against λ drops sharply through a second trim point where $\frac{\partial Q}{\partial \lambda} < 0$, and where the autorotation would be unstable.

Above a critical value of blade incidence the curve for Q against λ does not intersect the $Q = 0$ axis. Hence in this case there is no trim point, and no autorotation is possible.

Below the critical blade angle, where both trim points exist, autorotation can only be steady at the first, stable trim point. The slightest disturbance from the unstable trim state would either cause the rotor to revert to the first, stable trim state, or stop autorotating completely.

If the momentary increase in λ, due to an upgust hitting a rotor in stable autorotation at the first trim point, were sufficient to increase λ beyond the second trim point, the autorotation would stop. If the increase in λ were less than the difference in the two trim points, then the autorotation would return to the steady stable state at the first trim point.

In order to investigate the critical blade angle above which autorotation is impossible, and, for those blade angles where steady autorotation can exist, to predict the value of an upgust which would cause the autorotation to stop, it is necessary to include the effect of blade stalling in the expressions for drag and lift coefficients as functions of angle of attack. For this purpose, it is assumed that, below the stall, the drag coefficient is given by a cubic in angle of attack, instead of the usual quadratic, and that, above the stall, the drag and lift coefficients are constant at values denoted by c_{d_s} and c_{l_s}, respectively. Thus, below the stall,

$$c_{d_o}' = \delta_0' + \delta_1 \alpha_r + \delta_2 \alpha_r^2 + \delta_3 \alpha_r^3 \tag{15}$$

The blade station at which the stall begins is denoted x_s, and is given by

$$c_{l_{max}} = a\left(\theta + \frac{\lambda}{x_s}\right) \tag{16}$$

or

$$x_s = \frac{\lambda}{\frac{c l_{max}}{a} - \theta} \tag{16a}$$

For blades of constant chord, the torque equation is

$$\frac{2C_Q}{\sigma} = \int_{x_s}^{1.0} a\lambda x^2\left(\theta + \frac{\lambda}{x}\right)dx + \int_0^{x_s} c l_s \lambda x^2 dx - \int_{x_s}^{1.0} x^3\left[\delta_0' + \delta_1\left(\theta + \frac{\lambda}{x}\right) + \delta_2\left(\theta + \frac{\lambda}{x}\right)^2 + \delta_3\left(\theta + \frac{\lambda}{x}\right)^3\right]dx - \int_0^{x_s} \delta_s x^3 dx \tag{17}$$

As written above, the equation applies for $0 < x_s < 1.0$, which is the range of interest here. For θ = Constant (no twist), integrating equation (17) and substituting from equation (16a),

$$\frac{2C_Q}{\sigma} = C_4\lambda^4 + C_3\lambda^3 + C_2\lambda^2 + C_1\lambda + C_0 \tag{18}$$

where

$$C_4 = \frac{1}{4\left(\frac{c_{l_{max}}}{a} - \theta\right)^4}\left[\left(\delta_0' - \delta_s\right) + \delta_1\theta + \delta_2\theta^2 + \delta_3\theta^3\right] +$$

$$\frac{1}{3\left(\frac{c_{l_{max}}}{a} - \theta\right)^3}\left[\left(\delta_1 + c_{l_s}\right) + \left(2\delta_2 - a\right)\theta + 3\delta_3\theta^2\right] +$$

$$\frac{1}{2\left(\frac{c_{l_{max}}}{a} - \theta\right)^2}\left[\left(\delta_2 - a\right) + 3\delta_3\theta\right] + \frac{\delta_3}{\left(\frac{c_{l_{max}}}{a} - \theta\right)}$$

$$C_3 = -\delta_3$$

$$C_2 = \frac{1}{2}\left(a - \delta_2 - 3\delta_3\theta\right)$$

$$C_1 = \frac{1}{3}\left[-\delta_1 + \left(a - 2\delta_2\right)\theta - 3\delta_3\theta^2\right]$$

$$C_0 = -\frac{1}{4}\left(\delta_0' + \delta_1\theta + \delta_2\theta^2 + \delta_3\theta^3\right)$$

The values of λ for $Q = 0$, and the slope, $\frac{\partial Q}{\partial \lambda}$, at those trim points can best be investigated by calculating and plotting $\frac{2C_Q}{\sigma}$ as a function of λ for various values of θ.

SAMPLE CALCULATIONS

The physical properties for the helicopter chosen for the sample calculations are as follows:

$W = 2700$ pounds

$b = 3$

$R = 20$ feet

$c = 1.25$ feet (constant) $= c_e$

$a = 5.6$ per radian

$c_{d_o} = 0.0087 - 0.0216\alpha_r + 0.40\alpha_r^2$

Variable Induced Velocity

For illustrative purposes, a linear twist of -6° is chosen with $\theta_{0.75R} = 4^\circ$, so that, in degrees,

$$\theta = 8.5 - 6x$$

or, in radians,

$$\theta = 0.1483 - 0.1048$$

A value of $\left(\frac{V}{\Omega R}\right)_{Q=0}$ of 0.0750 is assumed.

Performing steps (1) through (3) in the section entitled "Solution with Variable Induced Velocity," the variation of λ_x with x is computed. For example, for $x = 0.6$, by equations (6),

$$p_1 = 0.788$$

$$p_2 = 0.0209$$

$$p_3 = 8.20$$

Since $x < p_1$, using equation (8),

$$\lambda_x = 0.0124$$

Graphical integration of equation (10), using the variation of λ_x computed, gives a net area for Q very nearly zero. Therefore the value of $\left(\frac{V}{\Omega R}\right)_{Q=0}$ is sufficiently accurate.

Graphical integration of equation (9) gives

$$\frac{T}{\frac{\rho}{2} ba\Omega^2 R^3} = 0.0385$$

whence $\Omega = 20.9$ radians per second. Then

$$V = \left(\frac{V}{\Omega R}\right)\Omega R = 31.3 \text{ feet per second}$$

At blade station $x = 0.6$, the blade angle of attack is

$$\alpha_r = \theta + \frac{\lambda_x}{x} = 8.5 - 6(0.6) + \frac{0.0124}{0.6}\,57.3 = 6.1^\circ$$

Constant Induced Velocity

For the same pitch and linear twist, using equations (13) through (13f),

$c_1 = 13.50$ $\qquad$ $c_5 = -0.00226$

$c_2 = 0.0233$ $\qquad$ $c_6 = 0.1190$

$c_3 = 0.50$ $\qquad$ $c_7 = 2.60$

From equation (14a),

$$\lambda = 0.0145$$

From equation (11),

$$\Omega = 21.0 \text{ radians per second}$$

$$u = \lambda\Omega R = 6.09 \text{ feet per second}$$

$$\overline{F} = \frac{T}{2\pi\rho R^2 u^2} = 12.2$$

From equation (1), using the plus sign and $K = 2$,

$$\frac{1}{\overline{f}} = 2.16$$

whence

$$V = \sqrt{\frac{T}{2\pi\rho R^2 \overline{f}}} = 31.2 \text{ feet per second}$$

At blade station $x = 0.6$, the angle of attack is

$$\alpha_r = \theta + \frac{\lambda}{x} = 8.5 - 6(0.6) + 57.3\,\frac{0.0145}{0.6} = 6.3^\circ$$

Stability of Autorotation

For this calculation the cubic drag polar is assumed,

$$c_{d_o}' = 0.0087 + 0.0600\alpha_r - 1.28\alpha_r^2 + 8.0\alpha_r^3$$

corresponding to

$$\delta_0' = 0.0087$$

$$\delta_1 = 0.0600$$

$$\delta_2 = -1.28$$

$$\delta_3 = 8.00$$

Values pertinent to stalling are taken to be

$$c_{l_{max}} = 1.20$$

$$c_{l_s} = 0.60$$

$$\delta_s = 0.250$$

Values of the coefficients C_4, C_3, C_2, C_1, and C_0 are computed for various values of θ, and the variation of $\frac{2C_Q}{\sigma}$ with λ is computed. Although these calculations are not given in detail, the results are presented in figure 3. The dashed lines are the curves of $\frac{2C_Q}{\sigma}$ against λ computed by equation (12) in which blade stalling is neglected. They are shown to indicate the effects of blade stalling, and to indicate the ranges of λ and θ where blade stalling may be neglected.

DISCUSSION OF CALCULATIONS

Comparison of Variable and Constant Induced-Velocity Theories

Calculations for rate of descent V and rotor speed Ω for the sample helicopter (see SAMPLE CALCULATIONS) have been carried out for different amounts of blade twist, by both constant and variable induced-velocity methods. The results, shown in figure 4, indicate that, for performance calculations, the results by the two methods are practically indistinguishable.

The variations of angle of attack along the blade, as computed for the above cases by the two methods, are plotted in figure 5. Although the agreement is good for negative twist, it is clear that the theoretical blade load distribution is, in general, considerably affected by the assumption of constant induced velocity.

Stability of Autorotation

The variation of $\frac{2C_Q}{\sigma}$ against λ for various values of θ, for the sample helicopter, is given in figure 3. The blade drag polar used for these calculations is compared with the quadratic expression (used in the other calculations) in figure 6. It will be noted that the two are essentially identical at low lift coefficients, but that at higher lift coefficients a more realistic increase in drag is given by the cubic expression used. Also, the stall is considered.

Consideration of figure 3 shows that for small blade incidence, the second, unstable trim point is far enough from the stable one that even a strong upgust would not cause λ to increase beyond it. At high values of incidence, however, the two trim points are so close together that a rotor in stable autorotation at the first point might become unstable, and stop autorotation, if hit by even a weak upgust, with its attendant momentary increase of λ.

There is, of course, a value of θ (about 8.8°, from the fig.) above which there is no trim point, and therefore autorotation is not possible. It is worth noting that using the quadratic drag polar, in which stall is neglected, not only results in failure to predict the second, unstable trim point and its attendant danger at high values of θ, but would also indicate that autorotation would be possible at any value of θ. It is apparent, then, that the blade stall cannot be neglected at high incidence.

In figure 7, values of λ for the first trim points are plotted against θ, as read from the curves of figure 3. For comparison, values

of λ computed by the method given in the section entitled "Solution with Induced Velocity Assumed Constant over the Disk," using the quadratic drag polar and neglecting the stall, are also shown. For small values of θ, the difference is very slight, indicating that blade stalling can safely be neglected for performance calculations at low incidence.

It should be noted that the results obtained from the study of stability of autorotation should be considered purely qualitative. The most important reason is that the constant induced-velocity theory used fails to predict accurately the angle-of-attack distribution along the blade, and hence cannot accurately account for the all-important distribution of stall at high angles of incidence where the stability is questionable. To be confident of quantitative results it would first be necessary, therefore, to predict accurately the actual induced-velocity distribution. It would also be necessary to represent accurately the drag curve at angles above the stall, and to account for Reynolds number effect on drag and maximum lift at various blade stations.

CONCLUSIONS

Although they are somewhat limited by the assumptions used in the theory on which they are based, the following conclusions seem justified:

1. Rate of descent and rotor speed are not critically affected by different assumptions for rotor thrust coefficient based on descending velocity $\overline{f}$ against rotor thrust coefficient based on resultant velocity $\overline{F}$ in the range of conditions encountered in steady autorotative descent.

2. For the computation of rate of descent and rotor speed, constant induced-velocity theory may be used at low incidence where stalling may be neglected. At high incidences, blade stalling must be accounted for in order to obtain even qualitative agreement between theory and practice. For quantitative agreement in this case, it would probably be necessary to use a variable induced-velocity theory.

3. At high values of incidence, although the autorotation may be stable for infinitesimal disturbances, a finite disturbance such as an upgust might well stall enough of the blades to put the rotor in an unstable regime where it would cease autorotating. There is little danger of this, at least for aerodynamically clean blades, at low incidence.

4. For the sample design studied, the constant induced-velocity theory, accounting for blade stalling, indicates a critical value of blade incidence of about 8.8°, above which steady autorotation would not be possible.

Princeton University
Princeton, N. J., May 4, 1948

REFERENCES

1. Glauert, H.: The Analysis of Experimental Results in the Windmill Brake and Vortex Ring States of an Airscrew. R. & M. No. 1026, British A.R.C., 1926.

2. Bennett, J. A. J.: Rotary-Wing Aircraft. Aircraft Eng., vol. XII, no. 12, 1940, pp. 40-42, 44.

3. Lock, C. N. H., Bateman, H., and Townend, H. C. H.: An Extension of the Vortex Theory of Airscrews with Applications to Airscrews of Small Pitch, Including Experimental Results. R. & M. No. 1014, British A.R.C., 1926.

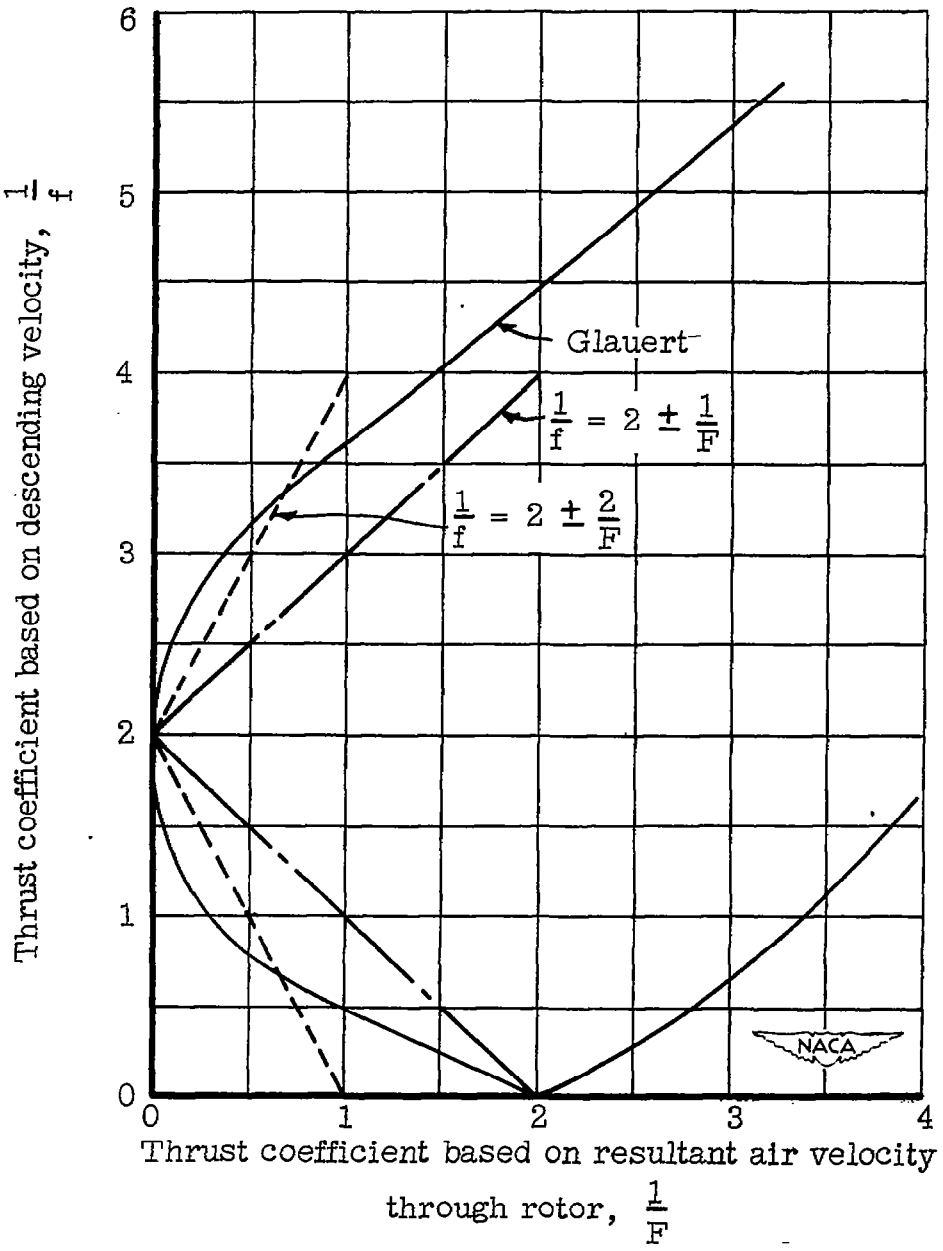

Figure 1.- Empirical relations between descending velocity V_v and resultant air velocity through the rotor U_p.

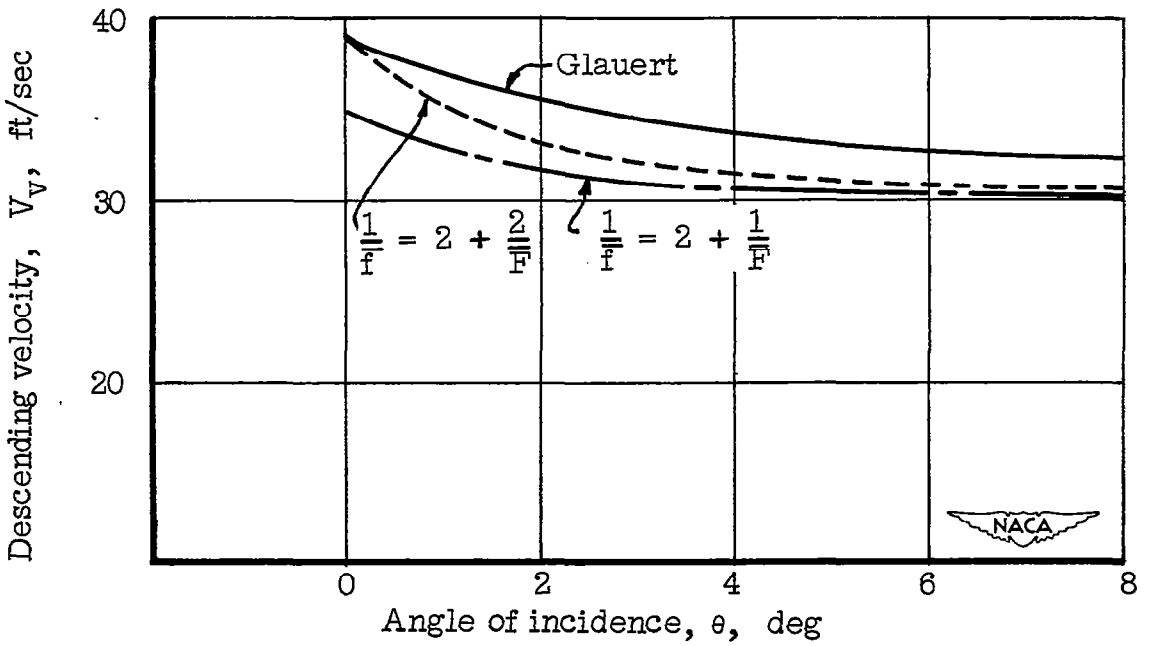

Figure 2.- Effect of different empirical relations for induced velocity on descending velocity in steady autorotation. Constant induced-velocity theory. No blade twist or taper. $c_1 = 13.50$; $c_{d_o} = 0.0087 - 0.0216\,\alpha_r + 0.40\,\alpha_r^2$.

Fig 4

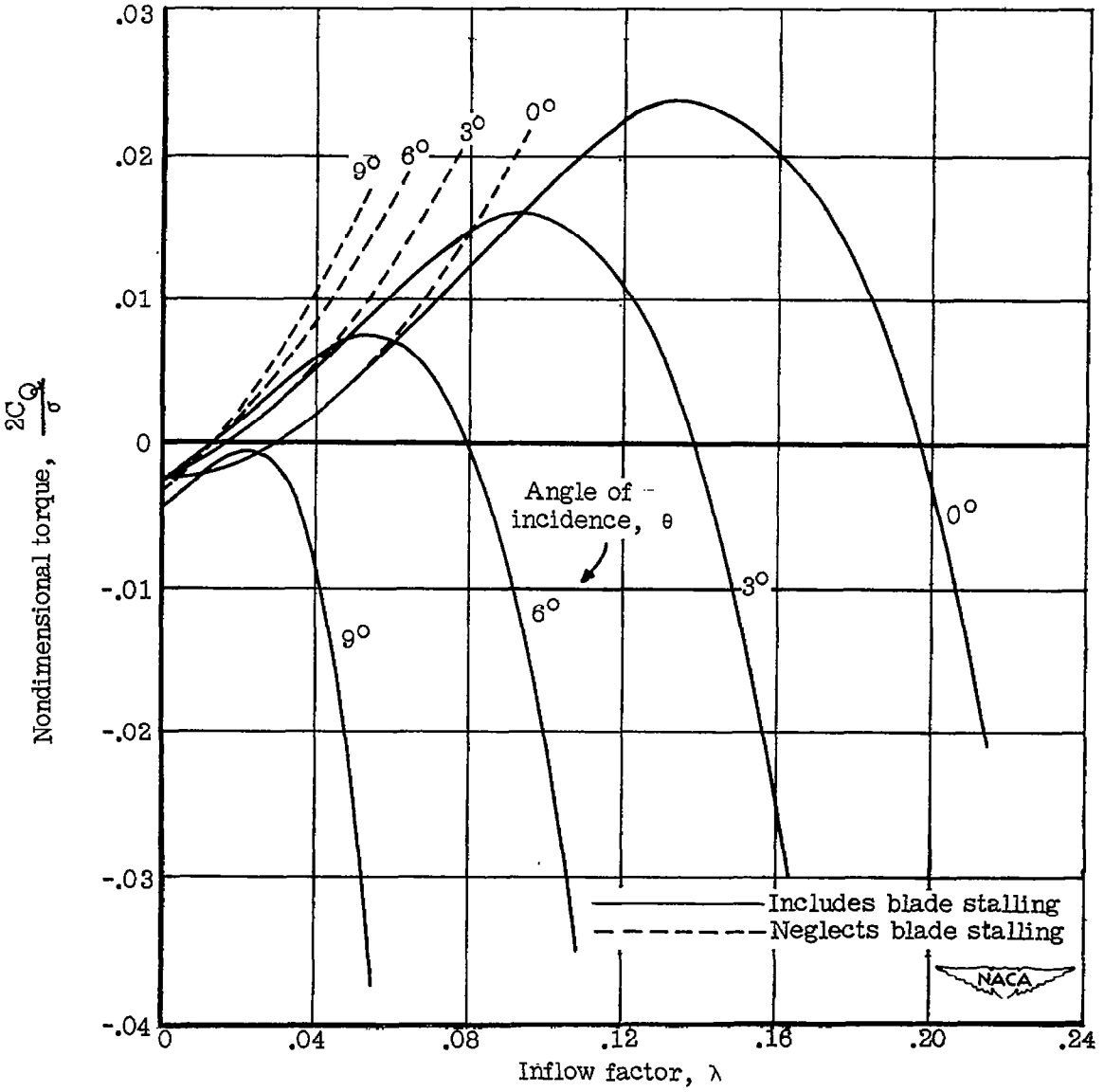

Figure 3.- Effect of neglecting blade stalling on aerodynamic torque against inflow factor λ for various angles of incidence.

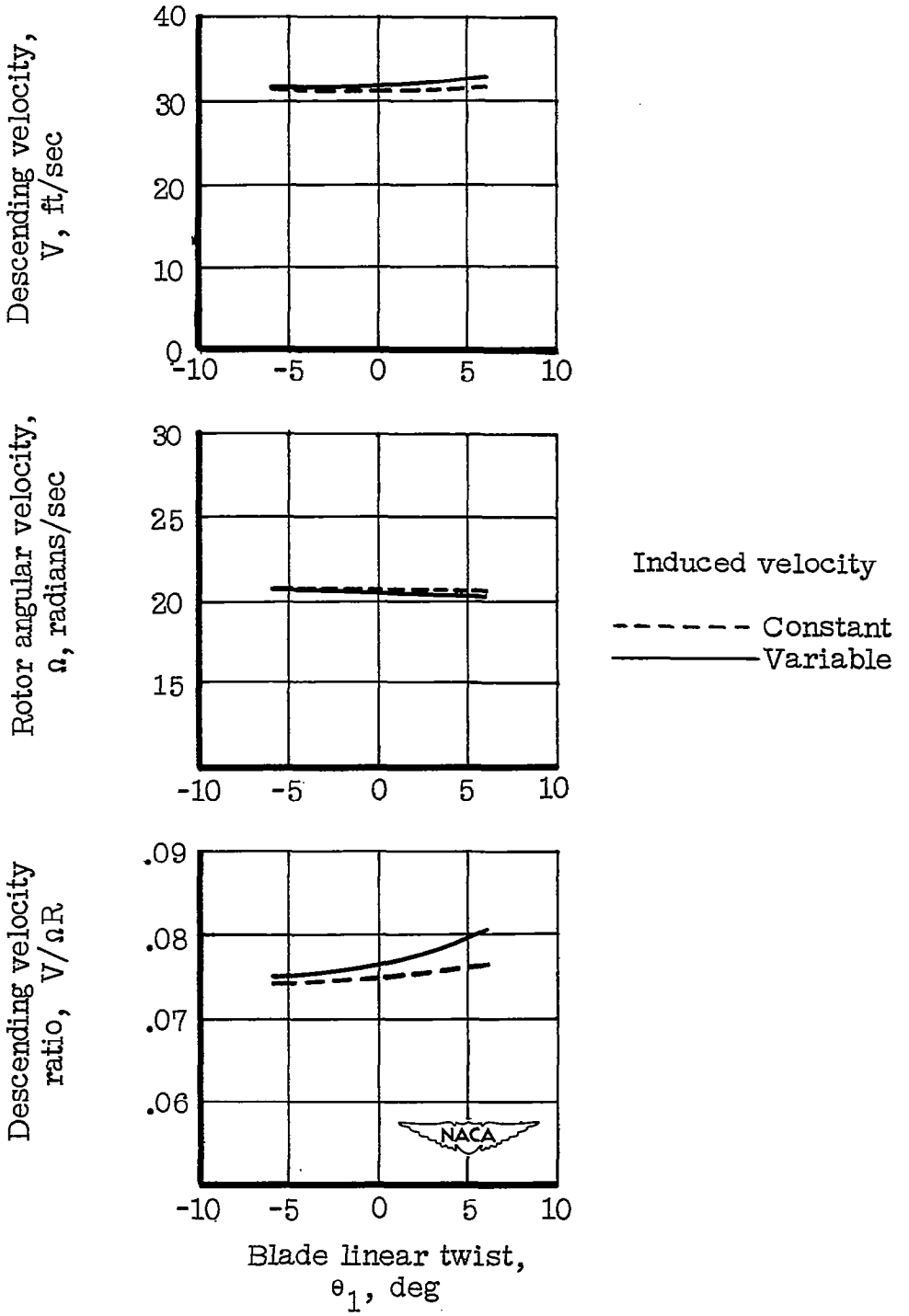

Figure 4.- Comparison of steady autorotation as computed by constant and variable induced-velocity theories. For all cases, $\theta_{0.75R} = 4^\circ$.

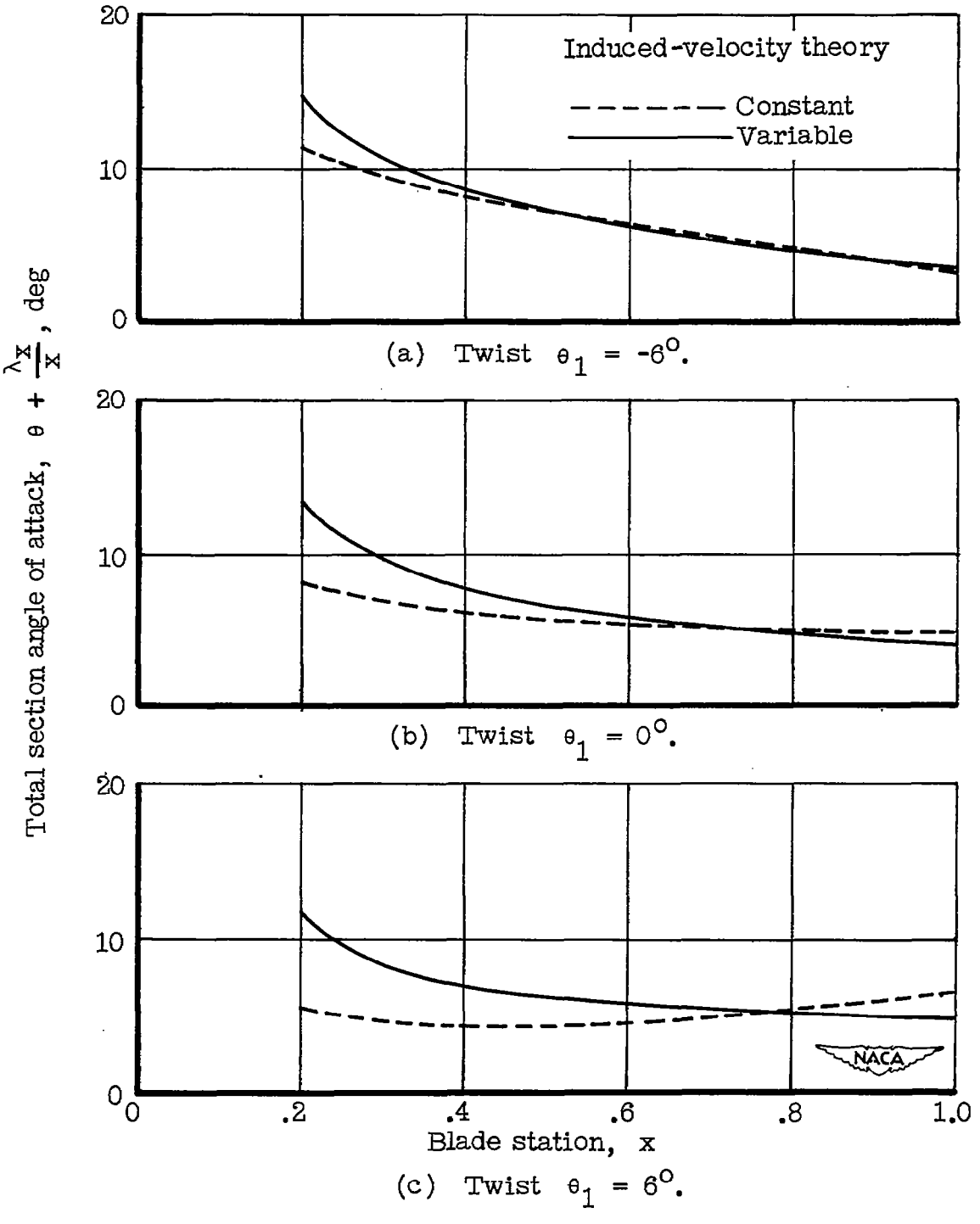

Figure 5.- Comparison of distribution of angle of attack in steady autorotation as computed by constant and variable induced-velocity theories. For all cases, $\theta_{0.75R} = 4^\circ$.

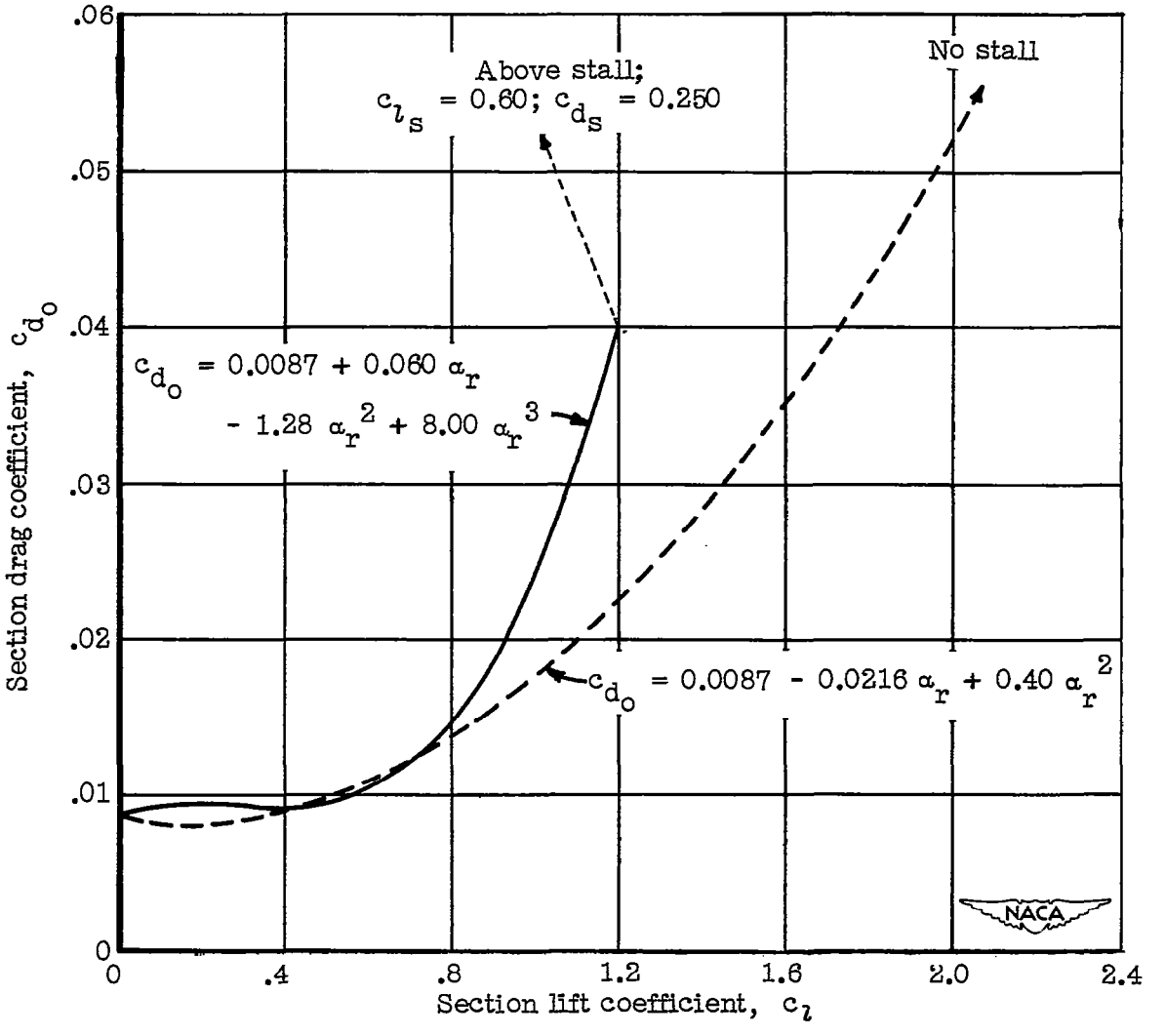

Figure 6.- Section drag polars (two different assumptions). a = 5.60 per radian.

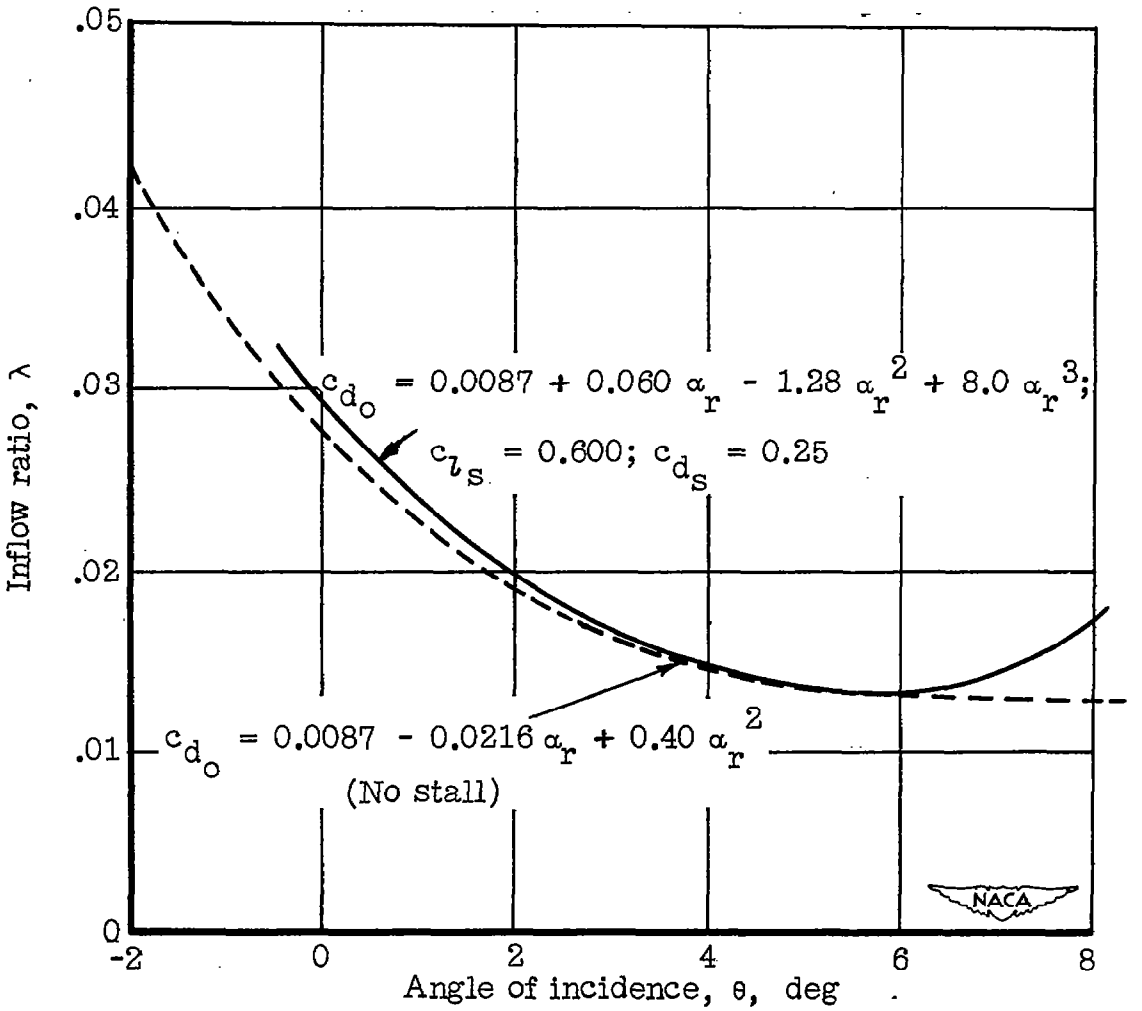

Figure 7.- Inflow ratio against incidence, as affected by blade stalling. No blade twist or taper. Constant induced-velocity theory.